JBC Papers in Press. Published on August 4, 2006 as Manuscript M605049200
The latest version is at http://www.jbc.org/cgi/doi/10.1074/jbc.M605049200

Characterization of Amyotrophic Lateral Sclerosis-Linked Pro56Ser Mutation of Vesicle-Associated Membrane Protein-Associated Protein B (VAPB/ALS8)

Kohsuke Kanekura[1, 2, 3], Ikuo Nishimoto[1], Sadakazu Aiso[2], and Masaaki Matsuoka[1, 4]

1. Department of Pharmacology and 2. Department of Anatomy, KEIO University School of Medicine, 35 Shinanomachi, Shinjuku-ku, Tokyo 160-8582 Japan
3. Japan Society for the Promotion of Science Research Fellow
4. corresponding author

Running Title: Characterization of ALS-linked P56S-VAPB

All correspondence should be addressed to Masaaki Matsuoka: Department of Pharmacology, KEIO University School of Medicine, 35 Shinanomachi, Shinjuku-ku, Tokyo 160-8582 Japan, Phone: +81-3-5363-8427; Fax: +81-3-5363-8428; E-mail: sakimatu@sc.itc.keio.ac.jp

The Pro56Ser (P56S) mutation in vesicle-associated membrane protein-associated protein B (VAPB) causes autosomal-dominant motoneuronal diseases (MNDs). Although it was reported that the P56S mutation induces localization shift of VAPB from endoplasmic reticulum (ER) to non-ER compartments, it remains unclear what the physiological function of VAPB is and how the P56S mutation in VAPB causes MNDs. Here we demonstrate that overexpression of wt-VAPB promotes unfolded protein response (UPR) which is an ER reaction to suppress accumulation of misfolded proteins and small interfering RNA for VAPB attenuates UPR to chemically induced ER stresses, indicating that VAPB is physiologically involved in UPR. The P56S mutation nullifies the function of VAPB to mediate UPR by inhibiting folding of VAPB that results in insolubility and aggregate formation of VAPB in non-ER fractions. Furthermore, we have found that expression of P56S-VAPB inhibits UPR, mediated by endogenous wt-VAPB, by inducing aggregate formation and mislocalization into non-ER fractions of wt-VAPB. Consequently, the P56S mutation in a single allele of the *VAPB* gene may diminish the activity of VAPB to mediate UPR to less than half the normal level. We thus speculate that the malfunction of VAPB to mediate UPR, caused by the P56S mutation, may contribute to the development of motoneuronal degeneration linked to VAPB/ALS8.

Amyotrophic lateral sclerosis (ALS) is the most prevalent fatal motor neuron disease, characterized by progressive loss of upper and lower motor neurons (1, 2). Although typical cases occur sporadically, some patients have a genetic background.

To date, four ALS-causative genes have been identified, and precise characterization of their physiological roles and abnormalities by ALS-causing mutations is bringing us clues as to how ALS and other

motor neuron diseases occur. Overexpression of mutants of Cu/Zn-superoxide dismutase (SOD1), whose gene is the most characterized familial ALS-related one known as *ALS1*, causes neuronal cell death *in vitro* (3, 4), and an ALS-like phenotype *in vivo* (5, 6). A recently identified autosomal-recessive ALS-causative gene, *ALS2*, encodes alsin protein (7, 8) that has several functional domains common to Rho guanine nucleotide exchanging factors (RhoGEF) (9) and Rab5GEF (10). We have recently demonstrated that alsin exerts neuroprotective function via its RhoGEF domain against neurotoxicity by SOD1 mutants *in vitro* (4). Ablation of the *ALS2* gene caused mild motor disorder (11). *ALS4*, a recently identified autosomal-dominant ALS-associated gene, is thought to encode a DNA/RNA helicase whose function remains unknown (12).

ALS8, encoding mutated vesicle-associated membrane protein-associated protein B (VAPB), was most recently identified from a large Brazilian family with autosomal-dominant motor neuron diseases. The P56S point mutation in VAPB caused a typical ALS phenotype with rapid progression or late-onset spinal muscular atrophy (SMA) (13). This mutation has affected eight families totaling 1500 individuals, of whom 200 suffer from ALS/SMA (14).

The human VAP family proteins were initially identified as homologues of vesicle-associated membrane protein (VAMP)-associated protein (VAP) with a size of 33kDa in Aplysia californica (aVAP33) (15) that is involved in exocytosis of neurotransmitters (16). They include VAPA (synonym, VAP33), VAPB, and VAPC. VAPB and VAPC are alternatively spliced variants. VAPA and VAPB, which interact with each other, associate with VAMP/synaptobrevin (15). It was subsequently demonstrated that the yeast VAP homologue, called suppressor of choline sensitivity 2 (*SCS2*), compensates for the defect of *IRE1* and *HAC1* (17). *IRE1* and *HAC1* encode yeast homologues of mammalian inositol requiring enzyme-1 (IRE1) and a mammalian transcriptional factor X-box binding protein-1 (XBP1). IRE1 and XBP1 play a pivotal role in inositol metabolism and unfolded protein response (UPR) (18), an ER process to suppress accumulation of unfolded protein in ER (19). Several other reports have also suggested that VAPB may play important roles in the structural regulation of ER, protein transport, phospholipids metabolism, and also viral infection (17, 20, 21).

Based on the foregoing studies, it is speculated that VAPB is involved in ER function, especially UPR induction mediated by the IRE1/XBP1 pathway, and in inositol metabolism (22, 23) although there is no direct evidence supporting this idea. Moreover, it remains unclear how the ALS-causing P56S-VAPB mutant participates in the pathomechanism of ALS. So far, the sole reported finding relating to the latter issue is that P56S-VAPB localizes in non-ER and non-Golgi compartments while wt-VAPB does so in ER and the Golgi apparatus (13).

In this study, we demonstrate that VAPB plays an important role in UPR. We further show that the P56S mutation causes almost complete loss of function of VAPB to mediate UPR by inducing its misfolding and localization shift to the non-ER compartments. In addition, P56S-VAPB suppresses UPR, mediated by wt-VAPB, by interfering with the folding of wt-VAPB. Inhibition of wt-VAPB-mediated UPR by co-expressed P56S-VAPB may occur possibly because wt-VAPB is firmly dimerized with P56S-VAPB and may be trapped into inactive homodimerized protein complexes. Taking altogether, we speculate that the function of VAPB to mediate UPR may be diminished to less than a half of the normal level by the

P56S mutation in a single allele of the *VAPB* gene. We further speculate that the malfunction of VAPB to mediate UPR, induced by the P56S mutation, may eventually contribute to the development of motoneuronal degeneration linked to ALS8 by permitting the accumulation of misfolded proteins in ER.

Experimental Procedure

Antibodies and compounds

Rabbit anti-VAPB polyclonal antibody was purchased from Abcam (Cambridge, UK). Immunoblot analysis with this antibody only detects overexpression levels of VAPB, but not endogenous levels of VAPB, in NSC34 cells. Rabbit polyclonal anti-VAPB-P antibody was raised against an N-terminal human VAPB peptide (N-terminal 14 residues) by Tanpaku Seisei Kogyo (Japan). Anti-FLAG-M2 beads consisting of anti-FLAG M2 monoclonal antibody, horseradish peroxidase (HRP) conjugated anti-FLAG M2 monoclonal antibody, and rabbit anti-actin polyclonal antibody were purchased from Sigma-Aldrich (St. Louis, MO). Mouse monoclonal anti-Xpress antibody and HRP conjugated anti-HisG antibody, which recognizes the N-terminal His6-Gly tag, were purchased from Invitrogen (Carlsbad, CA). HRP-conjugated goat anti-mouse secondary antibody and HRP-conjugated goat anti-rabbit secondary antibody were purchased from Bio-Rad (Hercules, CA). Rabbit polyclonal anti-Calreticulin antibody and anti-Calnexin antibody were purchased from Stressgen (Victoria, Canada). TexasRed conjugated goat anti-rabbit polyclonal antibody was purchased from Jackson ImmunoReseach Laboratories (West Grove, PA). The following mouse monoclonal antibodies were purchased from companies: anti-myc antibody, Biomol (Plymouth Meeting, PA); HRP-conjugated anti-HA antibody, Roche (Basel, Switzerland); anti-GST-antibody, Upstate (Charlottesville, VA); anti-tubulin antibody, Oncogene (Cambridge, MA). Thapsigargin, Bafilomycin A and Brefeldin A were purchased from Sigma-Aldrich. MG132 was purchased from Calbiochem (San Diego, CA).

Constructions

Human cDNAs encoding VAPB (GenBank accession no. **NM_004738**), VAPA (GenBank accession no. **BT019618**), VAMP1 (GenBank accession no. **NM_014231**) and VAMP2 (GenBank accession no. **NM_014232**) were amplified from a human postcentral gyrus cDNA library (Biochain, Hayward, CA) by polymerase chain reaction with a sense primer (5'-CGGGATCCACCAATGGCGAAGGTGGAGCAGGTC-3') and an antisense primer (5'-GGAATTCCTACAAGGCAATCTTCCCAATAATTAC-3') for human VAPB, a sense primer (5'-CGGGATCCACCATGGCGAAGCACGAGCAG-3') and an antisense primer (5'-GGAATTCCTACAAGATCAATTTCCCTAGAAAGAATC-3') for VAPA, a sense primer (5'-CGGGATCCACCATGTCTGCTCCAGCTCAGC-3') and an antisense primer (5'-GGAATTCAGTAAAAAAGTAGATTACAATAAACTACCACGATG-3') for VAMP1, and a sense primer (5'-CGGGATCCACCATGTCTGCTACCGCTG-3') and an antisense primer (5'-GGAATTCAGTGCTGAAGTAAACTATGATGATGATG-3') for VAMP2, respectively. Mouse VAPB cDNA (GenBank accession no. **NM_019806**) was amplified from mRNA of NSC34 cells by RT-PCR with a sense primer (5'-CGGGATCCACCATGGCGAAGGTGGAAC-3') and an anti-sense primer (5'-GGAATTCCTACAAGGCAATCTTCCCTATAATGAC).

P56S-VAPB, P56S-VAPA, P56A-VAPB, P56K-VAPB, P56D-VAPB, P56del-VAPB

and K87D/M89D-VAPB were obtained by site-directed mutagenesis with a sense primer (5'-GGTACTGTGTGAGGTCCAACAGCGGAATCATCG-3') and an antisense primer (5'-CGATGATTCCGCTGTTGGACCTCACACAGTACC-3') for P56S-VAPB and P56S-VAPA, a sense primer (5'-GGTACTGTGTGAGGGCCAACAGCGGAATCATCG-3') and an antisense primer (5'-CGATGATTCCGCTGTTGGCCCTCACACAGTACC-3') for P56A-VAPB, a sense primer (5'-GGTACTGTGTGAGGAAGAACAGCGGAATCATCG-3') and an antisense primer (5'-CGATGATTCCGCTGTTCTTCCTCACACAGTACC-3') for P56K-VAPB, a sense primer (5'-GGTACTGTGTGAGGGACAAACAGCGGAATCATCG-3') and an antisense primer (5'-CGATGATTCCGCTGTTGTCCCTCACACAGTACC-3') for P56D-VAPB, a sense primer (5'-GGTACTGTGTGAGGAACAGCGGAATCATCG) and an antisense primer (5'-CGATGATTCCGCTGTTCCTCACACAGTACC-3') for P56del-VAPB, a sense primer (5'-CCCAATGAGAAAAGTAAAACACGACTTTGACGTTCAGTCTATGTTTGCTCC-3') and an antisense primer (5'-GGAGCAAACATAGACTGAACGTCAAAGTCGTGTTTACTTTTCTCATTGGG-3') for K87D/M89D-VAPB, respectively.

Plasmid-based small interfering RNA for silencing of endogenous VAPB was constructed as follows. Two oligonucleotides, a sense fragment (5'-CGGGATCCCGTAGACTGAACCATAAACTTGTTTGATATCCGACAAGTTTATGGTTCAGTCTATTTTTTCCAAGGTACCCC-3') and an antisense fragment (5'-GGGGTACCTTGGAAAAAATAGACTGAACCATAAACTTGTCGGATATCAAACAAGTTTATGGTTCAGTCTACGGGATCCCG), were annealed *in vitro* and subcloned into BamHI-KpnI site of pRNA-U6.1/Shuttle vector (Genscript, New Jersey). pCAX-F-XBP1-Venus and pCAX-F-XBP1-ΔDBD-Venus constructs were kindly provided by Dr. Masayuki Miura (Tokyo Univ. Japan). pXJ-HA-ubiquitin plasmid was a kind gift from Dr. Victor Yu (National Univ. of Singapore).

Cell culture and transfection

Motoneuronal NSC34 cell, a hybrid cell line established from a mouse neuroblastoma cell line and mouse embryo spinal cord cells, was a kind gift from Dr. Neil Cashman (Toronto Univ. Canada). NSC34 cells were grown in Dulbecco modified Eagle's medium (DMEM) supplemented with 10% of fetal bovine serum (Hyclone, Logan, UT). NSC34 cells were seeded onto a 6-cm culture dish at $2.1x10^5$ cells/dish 24 hr before transfection. Transfection was performed under the manufacturer's protocol. In brief, DNA (3 μg), LipofectAMINE (6 μl), and PLUS reagent (12 μl) were premixed for each transfection. The premixed complexes were then added onto the cells cultured in serum-free DMEM, and 3 hr after transfection, the culture media were changed to 10%-FBS-DMEM.

Immunoblot analysis

Samples were mixed with equal amounts of 2x sample buffer containing 4% SDS and boiled for 5 min at 95°C. The samples were applied to sodium dodecyl-sulfate polyacrylamide electrophoresis (SDS-PAGE) and blotted onto polyvinylidene fluoride membranes. Immunoreactive bands were detected with ECL Western Blotting Detection Reagents (Amersham Bioscience, Uppsala, Sweden). Intensities of immunodetected signals were densitometrically estimated with " NIH image"

Immunocytochemistry

COS7 cells, plated onto cell culture dishes, were transfected with N-terminally EGFP-tagged VAPB by lipofection with LipofectAMINE and PLUS reagent. Forty-eight hr after transfection, the cells were fixed with 4% paraformaldehyde-PBS. ER was probed by anti-Calreticulin antibody (Stressgen) and visualized by TexasRed conjugated goat anti-rabbit antibody (Jackson ImmunoReseach Laboratories). The cells were observed with a confocal microscopy LSM510 (Carl Zeiss, Germany).

Pulldown assay

NSC34 cells, transiently expressing GST-fused proteins and His6-Xpress tagged proteins, were harvested 48 hr after transfection and lysed with a pulldown buffer [150 mM NaCl, 20 mM HEPES (pH 7.5), 1 mM EDTA, 1 mM dithiothreitol (DTT), 0.5% Triton-X 100, protease inhibitors] by pipetting and a freeze-thaw cycle. After centrifugation, the cell lysates were pre-cleared with sepharose beads for 4 hr, and pulled down with glutathione-sepharose beads (Amersham Bioscience) for 4 hr. After being washed 4 times with the pulldown buffer, the precipitates were immunoblotted with anti-HisG antibody (for the detection of His6-Xpress-tagged proteins) and anti-GST antibody.

Ubiquitination assay

NSC34 cells, cotransfected with the vector encoding HA-ubiquitin in association with the pEF4/His vector, pEF4/His-wt-VABP, or pEF4/His-P56S-VAPB, were harvested 48 hr after transfection for lysis with the RIPA buffer (1x PBS, 1% Nonidet P-40, 0.5% Sodium Deoxycholate, 0.1% SDS). The cell lysates were then pre-cleared with sepharose beads for 4 hr and immunoprecipitated with anti-Xpress antibody. After being washed 4 times with the RIPA buffer, the precipitates were immunoblotted with HRP conjugated anti-HA antibody (to detect ubiquitinated proteins) and anti-HisG antibody (to detect VAPB).

Fractionation into soluble and insoluble fractions

NSC34 cells overexpressing VAPB were harvested 48 hr after transfection for lysis with a cell lysis buffer [10 mM Tris-HCl (pH 7.4), 1% Triton-X100, 1mM EDTA, protease inhibitors] by pipetting and a freeze-thaw cycle. The soluble fraction was defined as the supernatant of the cell lysates after centrifugation at 12,000 g for 5 min. After complete removal of the supernatant, the pellets were resuspended in 500 μl of the cell lysis buffer and sonicated for 10 seconds to homogenize the mixture. The solutions were then centrifuged for 5 min at 12,000 g, and the supernatant was completely removed. The resulting pellets, defined as the insoluble fractions, were solubilized by pipetting in the 4% SDS-containing sample buffer for subsequent immunoblot analysis.

Fractionation by sucrose density gradient centrifugation

Untransfected NSC34 cells or NSC34 cells transfected with VAPB-encoding vectors were harvested for suspension in the 1% Triton-X100-MBS lysis buffer [1% Triton-X100, 25 mM MES (pH 6.7), 150mM NaCl] and rotated for 20 min at 4°C, followed by 10 passages through 26-gauge needles. The suspended total cell lysates, mixed with an equal volume of 80% sucrose-MBS (final 40% sucrose), were initially loaded to 4.5 ml ultracentrifuge tubes (Beckman, CA). A discontinuous sucrose gradient was then formed by sequentially layering 30% sucrose-MBS and 5% sucrose-MBS. After the tubes were subjected to ultracentrifugation at 260,000g for 18 hr in Beckman SW-Ti60 rotor at 4°C, the gradient was divided into the same volume (350 μl) of

fractions from the top to the bottom of the tube. The pellet was sonicated to suspend in 350 μl of the 1% TritonX-100-MBS lysis buffer. An equal volume (20 μl) of each fraction was then analyzed by Western blot.

RESULTS

The P56S mutation induces the insolubility of VAPB

We cloned a human wt-VAPB cDNA, from which the P56S-VAPB mutant cDNA was generated by site-directed mutagenesis (Fig. 1A). The 56th proline, located at the middle of the Major Sperm protein domain, is highly conserved among VAP family proteins derived from various species. We constructed their expression vectors to express various epitope-tagged proteins (Fig. 1B).

It has been generally accepted that many neurodegenerative-disease-linked mutations result in misfolding and aggregation of disease-related proteins (24-26). Misfolded proteins are prone to be easily polyubiquitinated (27, 28). To assess whether the P56S mutation induces misfolding and aggregation of VAPB, we first examined the status of polyubiquitination of P56S-VAPB. As shown in Figure 2A, P56S-VAPB was more ubiquitinated than wt-VAPB, supporting the idea that P56S-VAPB is also misfolded. Note that the expression level of P56S-VAPB is much lower than that of wt-VAPB in spite of transfection with same amount of plasmids.

Based on these findings, we tested whether the P56S mutation increased insolubility of VAPB in the Triton-X100-containing cell lysis buffer [1% Triton X-100, 10mM Tris-HCl (pH7.5), 1mM EDTA, protease inhibitors]. As shown in Fig. 2B, the amount of the Triton-X100-soluble P56S-VAPB was much smaller than that of Triton-X100-soluble wt-VAPB while the amount of the Triton-X100-insoluble P56S-VAPB was much greater than the Triton-X100-insoluble wt-VAPB. As expected, a smeared ladder, presumably composed of supershifted P56S-VAPB proteins, was detected in the insoluble fraction of P56S-VAPB. These higher-molecular-weight bands are assumed to be SDS-containing buffer-insoluble P56S-VAPB with some modifications or P56S-VAPB aggregates. Thus, it was concluded that the P56S mutation reduced the solubility of VAPB proteins by inducing misfolding of VAPB protein. Considering that VAPB is homodimerized or heterodimerized with other synaptic proteins via the C-terminal transmembrane domain (TMD) (15, 21) and that the P56S mutation does not interfere with this oligomerization (data not shown, but see Fig. 6), VAPB-interacting proteins may be trapped into insoluble aggregates of P56S-VAPB and contribute to the VAPB-containing smeared ladder.

P56S-VAPB shows different subcellular localization

wt-VAPB has been known to mainly localize in ER (13, 20, 21). It has been also demonstrated that the P56S-VAPB mutant does not co-localize with the Golgi apparatus or ER (13). To visualize these proteins *in situ*, we constructed enhanced green fluorescent protein (EGFP)-tagged VAPB. As shown in Fig. 2C, EGFP-wt-VAPB showed reticulated structures co-localizing with calreticulin, an ER marker. On the other hand, P56S-VAPB that showed fine dot-like structure did not co-localize with ER (Fig. 2D).

It has been known that some synaptic vesicular proteins, such as VAMP2, are known to localize in a scattered membrane fraction, called “raft” (30). Raft is known to be insoluble in the Triton X100-containing buffer. Taken altogether, it is possible that a minor portion of wt-VAPB, a putative synaptic vesicular protein, may localize in the

membrane raft and the P56S mutation may enhance the localization of VAPB in the membrane raft. To examine the possibility that the P56S mutation abnormally enhance the localization of VAPB into the membrane raft and to confirm the subcellular localization pattern of wt-VAPB and P56S-VAPB, we fractionated these proteins by sucrose density gradient centrifugation in the Triton X100-containing buffer (30).

For this purpose, untransfected NSC34 cells or NSC34 cells transfected with pEF4/His-wt-VAPB or pEF4/His-P56S-VAPB were harvested for suspension and homogenization in the Triton-X100-MBS buffer and the total lysates were then subjected to sucrose density gradient centrifugation. As shown in Fig. 2E, most endogenous wt-VAPB was distributed in 40% sucrose fractions. The fractionation pattern of endogenous wt-VAPB was almost equal to that of calnexin, an ER membrane protein, and calreticulin, a soluble ER protein (Fig. 2E, bottom). Overexpressed wt-VAPB showed the same fractionation pattern as endogenous wt-VAPB (Fig. 2F). Similar to other synaptic vesicular proteins such as VAMP2, a minor portion of wt-VAPB was distributed in several consecutive fractions around the border between 5% and 30% sucrose, suggesting that the minority of VAPB localizes in the Triton-X100-insoluble membrane raft fraction. In contrast, a major part of P56S-VAPB was fractionated into the Triton-X100-insoluble pellet (Fig. 2G), but not into the Triton-X100-insoluble raft, indicating that the P56S mutation induced the localization shift of VAPB into the non-ER and non-raft Triton-X100-insoluble subcellular compartments.

Overexpression of wt-VAPB, but not that of P56S-VAPB, induces unfolded protein response (UPR)

Several groups have predicted the involvement of mammalian VAP as well as SCS2 in UPR, in addition to inositol metabolism (22, 23). Based on these predictions, we hypothesized that VAPB may be involved in UPR and the P56S mutation may affect it.

In this study, to monitor UPR, we used a tool developed by Iwawaki et al. (29) (Fig. 3). Under the normal condition, mRNA of XBP1 is immature and Venus, a fluorescent protein, is not expressed because there is a stop codon just upstream of the Venus cDNA. Under the ER stress condition, IRE1 is activated and splicing of XBP1 occurs, followed by expression of XBP1-Venus fluorescent fusion proteins. It was confirmed that ER stress, but not other stresses, induced expression of XBP1-Venus (29). In accordance, as shown in Fig. 4A and 4B, treatment with Thapsigargin, which releases calcium from the ER followed by induction of ER stress, induced expression of fluorescent XBP1-Venus in NSC34 cells transfected with pCAX-F-XBP1-ΔDBD-Venus, indicating that the assay system worked appropriately.

Immunoblot analysis indicated that overexpression of wt-VAPB triggered expression of fluorescent XBP1-Venus protein (Fig. 4A, lane 4), whose expression was also confirmed by Venus fluorescence (Fig. 4B, wt). In contrast, expression of P56S-VAPB was unable to induce UPR when the same amount of plasmid was transfected (Fig. 4A and 4B, P56S). Note again that the major fraction of P56S-VAPB was insoluble in the non-ER compartments (Fig. 4A, insoluble VAPB).

In a similar fashion, overexpression of wt-VAPA, but not that of P56S-VAPA, triggered UPR (data not shown). In contrast, overexpression of the other synaptic vesicular proteins, VAMP1 or VAMP2, was unable to induce UPR (Fig 4C and 4D), indirectly indicating that overexpressed wt-VAPB-mediated induction of UPR did not occur due to the simple

overload of a synaptic vesicular protein but mimicked physiological UPR that may be mediated by wt-VAPB.

To examine the significance of the proline residue at the 56th position of VAPB in UPR induction, we performed a UPR induction assay using several VAPB mutants whose 56th amino acid was replaced. As shown in Fig. 4E, no tested P56X-VAPB derivative [Pro56Ser, Pro56Ala, Pro56Lys, and Pro56Asp] nor Pro56del-VAPB (proline at the 56th position is deleted) triggered UPR. In agreement, all of them showed increased Triton-X100 insolubility (Fig. 4E, bottom). These data support our hypothesis that the proline residue at the 56th position is essential for UPR induction by VAPB. In accordance, we recognized by immunofluorescence studies that P56A-VAPB or Pro56del-VAPB shows non-ER localization that is similar to that of P56S-VAPB (Fig. 4F). We also recognized that any other tested P56X-VAPB mutants showed subcellular localization almost similar to P56S- or P56A-VAPB.

Two amino acid substitutions of Scs2p and VAPA (K84D/L86D for Scs2p or K87D/M89D for VAPA), yeast and mammalian homologues of aVAP33, respectively, appear to cause loss of their function (31). As shown in Fig. 4E, overexpression of K87D/M89D-VAPB did not trigger UPR although it did not lose Triton-X100 solubility. This finding again supports the idea that UPR, induced by overexpression of wt-VAPB, did not occur due to the simple overload of a synaptic vesicular protein but mimicked physiological wt-VAPB-mediated UPR.

VAPB is involved in physiological UPR to chemically induced ER stresses.

For further investigation of the involvement of VAPB in UPR, we examined the effect of knockdown of endogenous VAPB expression with small interfering RNA for VAPB (siVAPB) on UPR to chemically induced ER stresses. NSC34 cells were cotransfected with pCAX-F-XBP-1-ΔDBD together with the pRNA-U6.1/Shuttle vector or pRNA-U6.1/Shuttle-siVAPB. Forty-eight hr after transfection, they were co-incubated with inducers of ER stresses, 1mM DTT or 100 nM Thapsigargin for 6hr. As shown in Fig. 5A and 5B, introduction of siVAPB attenuated UPR to ER stress caused by DTT or Thapsigargin in a fashion dependent on the decreased expression levels of endogenous VAPB, supporting the notion that VAPB is involved in UPR. Note that expression of endogenous VAPB was efficiently suppressed by siVAPB (Fig. 5A, middle panel). The siVAPB-mediated downregulation of UPR was confirmed with a Venus-immunofluorecence study (Fig 5C).

P56S-VAPB keeps its ability to interact with synaptic vesicular proteins, including wt-VAPB.

VAPB has been known to be homodimerized or heterodimerized with VAPA, another homologue of aplysia VAP33. It also associates with VAMP/synaptobrevins, synaptic vesicle proteins (15). We next asked how the homodimerization of VAPB is modified by the P56S mutation. To this end, NSC34 cells, cotransfected with the vector encoding glutathione-S-transferase (GST), GST-wt-VAPB, or GST-P56S-VAPB in association with the vector encoding His6-Xpress-wt-VAPB or His6-Xpress-P56S-VAPB, were harvested for pulldown analysis at 48 hr after transfection. As shown in Fig. 6A, P56S-VAPB was co-precipitated with wt-VAPB and P56S-VAPB. We next examined whether the heterodimerization of VAPB with VAPA was affected by the P56S mutation of VAPB. As shown in Fig. 6B, P56S-VAPB was also co-precipitated with wt-VAPA and P56S-VAPA. We further demonstrated that P56S-VAPB as well as wt-VAPB interacted with GST-VAMP1 or GST-VAMP2 (Fig.6C). We thus concluded that

P56S-VAPB keeps its ability to be homodimerized or heterodimerized with other synaptic vesicular proteins.

P56S-VAPB inhibits wt-VAPB-mediated UPR by inducing the insolubility of wt-VAPB.

It thus appears that the P56S-VAPB mutant is a loss-of-function mutant in induction of UPR (Fig. 4). On the other hand, P56S-VAPB kept its ability to interact with wt-VAPB and also other synaptic vesicular proteins (Fig. 6). Considering that P56S-VAPB tends to be highly insoluble and wt-VAPB and the other synaptic vesicular proteins are dimerized with P56S-VAPB, we hypothesized that wt-VAPB and the other synaptic vesicular proteins may be trapped into the insoluble fraction composed of P56S-VAPB and may lose their normal function when they are co-expressed.

To test this hypothesis, we examined whether P56S-VAPB altered the solubility of wt-VAPB or other synaptic vesicular proteins when they were co-expressed. As shown in Fig. 7A, co-expression of P56S-VAPB increased the amount of the insoluble His6-Xpress-tagged wt-VAPB and resulted in high-molecular-weight aggregates of wt-VAPB that were similar to misfolded and insoluble P56S-VAPB (Fig. 2B). In contrast, increase in insolubility and misfolding of wt-VAPA, VAMP1, or VAMP2 was not induced by co-expression of P56S-VAPB (Fig. 7B, 7C, and 7D), indicating that co-expression of P56S-VAPB specifically increases misfolding and insolubility of wt-VAPB. We have also demonstrated that any P56X-VAPB derivative (P56S, P56A, P56K, or P56D) or P56del-VAPB, but not K87D/M89D-VAPB, insolubilized co-expressed wt-VAPB, as shown in Fig. 7E.

To confirm this notion, we further performed sucrose density gradient centrifugation to investigate how P56S-VAPB captures co-expressed wt-VAPB. As shown in Fig. 7F, when cotransfected with the backbone vector, wt-VAPB co-distributed with ER proteins, represented by calreticulin and calnexin. However, when cotransfected with P56S-VAPB, a considerable portion of wt-VAPB was distributed in the pellet fraction (Fig. 7G), supporting the notion that P56S-VAPB interferes with the wt-VAPB function by inducing the insolubility and misfolding of wt-VAPB as well as the localization shift of wt-VAPB to the non-ER and non-raft compartments. Immunofluorescence studies have confirmed that co-expression of P56S-VAPB induced localization shift of a considerable portion of wt-VAPB from ER to non-ER compartments (Fig 7H).

Such effect of P56S-VAPB on the co-expressed wt-VAPB thus appears to reduce the wt-VAPB function dominant-negatively. To test this idea, NSC34 cells were cotransfected with the pEF1-vector or pEF1-P56S-VAPB in association with pCAX-F-XBP1-ΔDBD. Forty-eight hr after transfection, they were incubated with 100 nM Thapsigargin for 6hr. Subsequent UPR analysis indicated that UPR to Thapsigargin-induced ER stress was attenuated, once NSC34 cells were transfected with P56S-VAPB (Fig. 8A and 8B), supporting the idea that P56S-VAPB suppressed UPR, mediated by wt-VAPB, in a dominant-negative manner.

The P56S mutation affects the homodimerization of VAPB

As shown in Fig. 7, P56S-VAPB specifically affects the insolubility of co-expressed wt-VAPB, but not that of wt-VAPA, VAMP1 or VAMP2. We therefore speculated that the protein-protein interaction mechanism underlying the VAPB homodimerization may be different from that underlying the heterodimerization between VAPB and any other synaptic vesicular protein. Several groups have demonstrated that a deletion of

the C-terminal TMD from VAPB disables homodimerization or heterodimerization with other synaptic vesicle proteins (15, 21). We have observed that the deletion of C-terminal TMD disables VAPB from localizing in the membrane of ER or the Golgi apparatus (unpublished data). Therefore, it is possible that the deletion of C-terminal TMD attenuates the homodimerization or the heterodimerization by precluding proper localization of VAPB in the membrane of ER or the Golgi apparatus. As shown in Fig. 9A, however, we have also recognized that there is a weak interaction between wt-VAPB-ΔTMD and wt-VAPB, suggesting that VAPB may also form a homooligomer via sites other than the TMD. Furthermore, the P56S mutation of VAPB-ΔTMD dramatically enhanced the dimerization between P56S-VAPB-ΔTMD and P56S-VAPB (Fig. 9B) while it did not induce a similar effect for the dimerization between P56S-VAPB-ΔTMD and VAMP1 or VAMP2 (Fig. 9C). These data suggest that the P56S mutation may enable VAPB to form a stronger and more specific homodimer via the non-TMD site.

DISCUSSION

Elucidation of disease-causative abnormalities as well as the normal functions of ALS-linked genes has been steadily helping to understand the pathomechanisms underlying ALS. In this study, we have demonstrated that overexpression of wt-VAPB triggers UPR, and siRNA-mediated knockdown of endogenous VAPB expression attenuates IRE1/XBP1 signaling, triggered by DTT or Thapsigargin. These findings strongly support the notion that VAPB is physiologically involved in UPR. The P56S mutation in the *VAPB/ALS8* gene causes the insolubility in the Triton-X100-containing lysis buffer and the localization shift of VAPB to non-ER compartments. As a result, it causes loss of function to induce UPR. Furthermore, P56S-VAPB enhances misfolding of co-expressed wt-VAPB, and attenuates endogenous VAPB-mediated UPR. Taking together these findings and the clinical finding indicating that P56S-VAPB/ALS8 causes autosomal-dominant ALS/SMA, we could hypothesize that overall malfuction of VAPB-mediated UPR, caused by the P56S mutation in a single allele, may eventually lead to the abnormal accumulation of misfolded proteins in ER that contributes to the development of motoneuronal cell death related to *ALS8*. However, it is also possible that the loss of VAPB function in UPR by the P56S mutation may be unrelated to the onset of ALS/SMA. In the latter case, it should be hypothesized that the P56S mutation causes gain of a new neurotoxic function. This issue should be addressed in future investigations.

In mammalian cells, there are three major UPR pathways: PERK, ATF6, and IRE1/XBP1 pathways (32). The IRE1/XBP1 (*IRE1/HAC1* in yeast) pathway, the most conserved UPR pathway from yeast to mammals, increases protein chaperone expression and lipid synthesis (19). Based on the observations-IRE1 plays an essential role in both UPR induction and inositol metabolism (33); disruption of either IRE1 or HAC1 causes inositol auxotrophy (34, 35); overexpression of the yeast VAP homologue protein, Scs2p, can rescue the inositol auxotrophy by *IRE1/HAC1* mutants (36); and mature XBP1 increases lipid production (36)-it has been assumed that there is a close relationship between UPR and lipid metabolism and that VAPB functionally associates with IRE1/XBP1 signaling. In support of this notion, it was reported that deprivation of inositol triggers UPR in yeast cells (38) and that SCS2 and HAC1 functionally interact with each other under the UPR-inducing condition (38). Considering that VAPA interacts with ORPs, (22, 39-41) and yeast Scs2p interacts with yeast oxysterol-binding protein homologues,

Osh1p and Osh2p (42), we speculate that ORPs may be involved in VAPB-mediated UPR. The FFAT motif, whose consensus amino acid sequence is EFFDAXE, is conserved in a large protein family of ORPs. As shown in Fig. 4E, the K87D/M89D mutation that has been demonstrated to prevent VAP and SCS2 from interacting with the FFAT-motif-containing protein, resulting in loss of their functions (31), inhibited VAPB from triggering UPR, supporting our hypothesis. It was also reported that constitutive interaction between VAPA and OSBP, induced by a mutation in OSBP, causes accumulation of unfolded proteins and ceramide in ER (22).

Amino acid substitution analysis demonstrated the importance of the proline residue at the 56th position for the function and the localization of VAPB. Based on the fact that the proline residue is an imino acid that restricts the flexibility of the peptide chain and plays a pivotal role in the correct conformation of the protein, an amino substitution of proline residue often causes a drastic conformational change, promoting functional abnormalities (43, 44). Therefore, it is assumed that the replacement or the deletion of the proline residue at the 56th position in VAPB probably causes abnormal protein folding and insolubility that results in the localization shift to the non-ER fraction.

We also found a unique dominant-negative effect of P56S-VAPB. It insolubilizes co-expressed wt-VAPB and weakens UPR, mediated by endogenous wt-VAPB (Fig.7 and Fig. 8). By sucrose density gradient fractionation analysis and immunofluorescence analysis, we have confirmed that P56S-VAPB causes a shift of co-expressed wt-VAPB to the Triton-X100-insoluble non-ER fraction (Fig. 7G). Such insolubilization of co-expressed proteins specifically occurs when wt-VAPB, but not VAPA, VAMP1 or VAMP2, is co-expressed with P56S-VAPB (Fig. 7A B, C, and D). Based on the finding that the P56S mutation enhanced the homodimerization of VAPB via the non-TMD site (Fig. 9B), we speculate that the dimerization between P56S-VAPB and wt-VAPB may be also specifically enhanced in a manner different from the homodimerization mediated through the C-terminal TMD. However, because it is extremely difficult to increase the expression level of soluble P56S-VAPB to the level of soluble wt-VAPB, this idea has not experimentally proved.

The molecular mechanism underlying P56S-VAPB-induced motoneuronal death remains completely unknown. A straightforward hypothesis is that the malfunction of VAPB, induced by the P56S mutation, causes insufficient UPR induction, resulting in accumulation of misfolded proteins that may be toxic to motoneuronal cells in some situations. We need further *in vitro* and *in vivo* investigations to address the question as to whether and how the insufficiency of VAPB functions is linked to motoneuronal degeneration.

REFERENCES

1. Cleveland, D. W. and Rothstein, J. D. (2001) *Nat. Rev. Neurosci.* 2, 806-819
2. Bruijn, L. I., Miller, T. M., Cleveland, D. W. (2004) *Annu. Rev. Neurosci.* 27, 723-749
3. Ghadge, G. D., Lee, J. P., Bindokas, V. P., Jordan, J., Ma, L., Miller, R. J. and Roos, R. P. (1997) *J. Neurosci.* 17, 8756-8766

4. Kanekura, K., Hashimoto, Y., Niikura, T., Aiso, S., Matsuoka, M. and Nishimoto, I. (2004) *J. Biol. Chem.* 279, 19247-19256
5. Gurney, M. E., Pu, H., Chiu, A. Y., Dal Canto, M. C., Polchow, C. Y., Alexander, D. D., Caliendo, J., Hentati, A., Kwon, Y. W., Deng, H. X., Chen, W., Zhai, P., Sufit, R. L. and Siddique, T. (1994) *Science* 264, 1772-1775
6. Chiba, T., Hashimoto, Y., Tajima, H., Yamada, M., Kato, R., Niikura, T., Terashita, K., Schulman, H., Aiso, S., Kita, Y., Matsuoka, M. and Nishimoto, I. (2004) *J. Neurosci. Res.* 78, 542-552
7. Hadano, S., Hand, C. K., Osuga, H., Yanagisawa, Y., Otomo, A., Devon, R. S., Miyamoto, N., Showguchi-Miyata, J., Okada, Y., Singaraja, R., Figlewicz, D. A., Kwiatkowski, T., Hosler, B. A., Sagie, T., Skaug, J., Nasir, J., Brown, R. H., Jr., Scherer, S. W., Rouleau, G. A., Hayden, M. R. and Ikeda, J. E. (2001) *Nat. Genet.* 29,166-173
8. Yang, Y., Hentati, A., Deng, H. X., Dabbagh, O., Sasaki, T., Hirano, M., Hung, W. Y., Ouahchi, K., Yan, J., Azim, A. C., Cole, N., Gascon, G., Yagmour, A., Ben-Hamida, M., Pericak-Vance, M., Hentati, F. and Siddique, T. (2001) *Nat. Genet.* 29, 160-165
9. Kanekura, K., Hashimoto, Y., Kita, Y., Sasabe, J., Aiso, S., Nishimoto, I. and Matsuoka, M. (2005) *J. Biol. Chem.* 280, 4532-4543
10. Otomo, A., Hadano, S., Okada, T., Mizumura, H., Kunita, R., Nishijima, H., Showguchi-Miyata, J., Yanagisawa, Y., Kohiki, E., Suga, E., Yasuda, M., Osuga, H., Nishimoto, T., Narumiya, S. and Ikeda, J. E. (2003) *Hum. Mol. Genet.* 12, 1671-1687
11. Hadano, S., Benn, S. C., Kakuta, S., Otomo, A., Sudo, K., Kunita, R., Suzuki-Utsunomiya, K., Mizumura, H., Shefner, J. M., Cox, G.A., Iwakura, Y., Brown, R. H., Jr. and Ikeda, J. E. (2006) *Hum. Mol. Genet.* 15, 233-250
12. Chen, Y. Z., Bennett, C. L., Huynh, H. M., Blair, I. P., Puls, I., Irobi, J., Dierick, I., Abel, A., Kennerson, M. L., Rabin, B. A., Nicholson, G. A., Auer-Grumbach, M., Wagner, K., De Jonghe, P., Griffin, J. W., Fischbeck, K. H., Timmerman, V., Cornblath, D. R. and Chance, P. F. (2004) *Am. J. Hum. Genet.* 74, 1128-1135
13. Nishimura, A. L., Mitne-Neto, M., Silva, H. C., Richieri-Costa, A., Middleton, S., Cascio, D., Kok, F., Oliveira, J. R., Gillingwater, T., Webb, J., Skehel, P. and Zatz, M. (2004) *Am. J. Hum. Genet.* 75, 822-831
14. Nishimura, A. L., Al-Chalabi, A. and Zatz, M. (2005) *Hum. Genet.* 118, 499-500
15. Nishimura, Y., Hayashi, M., Inada, H. and Tanaka, T. (1999) *Biochem. Biophys. Res. Commun.* 254, 21-26
16. Skehel, P. A., Martin, K. C., Kandel, E. R. and Bartsch, D. (1995) *Science* 269, 1580-1583
17. Kagiwada, S., Hosaka, K., Murata, M., Nikawa, J. and Takatsuki, A. (1998) *J. Bacteriol.* 180,1700-1708
18. Calfon, M., Zeng, H., Urano, F., Till, J. H., Hubbard, S. R., Harding, H. P., Clark, S.G. and Ron, D. (2002) *Nature* 415, 92-96
19. Kaufman, R.J. (1999) *Genes Dev.* 13, 1211-1233

20. Amarilio, R., Ramachandran,S., Sabanay, H. and Lev S. (2005) *J. Biol. Chem.* 280, 5934-5944
21. Hamamoto, I., Nishimura, Y., Okamoto, T., Aizaki, H., Liu, M., Mori, Y., Abe, T., Suzuki, T., Lai, M. M., Miyamura, T., Moriishi, K. and Matsuura, Y. (2005) *J. Virol.* 79, 13473-13482
22. Wyles, J. P., McMaster, C. R. and Ridgeway, N. D. (2002*.) J. Biol. Chem.* 277, 29908-29918
23. Kagiwada, S. and Zen, R. (2003) *J. Biochem.* 133, 515-522
24. Bruijn, L. I., Houseweart, M. K., Kato, S., Anderson, K. L., Anderson, S. D., Ohama, E., Reaume, A. G., Scott, R. W. and Cleveland, D. W. (1998) *Science* 281, 1851-1854
25. Bates, G. (2003) *Lancet.* 361, 1642-1644
26. Shults, C. W. (2006) *Proc. Natl. Acad. Sci. U. S. A.* 103, 1661-1668
27. Obata, Y., Niikura, T., Kanekura, K., Hashimoto, Y., Kawasumi, M., Kita, Y., Aiso, S., Matsuoka, M. and Nishimoto, I. (2005) *J. Neurosci. Res.* 81, 720-729
28. Urushitani, M., Kurisu, J., Tsukita, K. and Takahashi R. (2002) *J. Neurochem.* 83, 1030-1042
29. Iwawaki, T., Akai, R., Kohno, K. and Miura, M. (2004) *Nat. Med.* 10, 98-102
30. Chamberlain, L.H. and Gould, G.W. (2002) J. Biol. Chem. 277, 49750-49754
31. Kaiser, S. E., Bricker, J. H., Reilein, A. R., Fenn, T. D., Walter, P and Brunger, A. T. (2005) Structure. 13, 1035-1045
32. Wu, J. and Kaufman, R. J., (2006) *Cell Death Differ.* 13, 374-384
33. Cox, J. S., Shamu, C. E. and Walter, P. (1993) *Cell* 73, 1197-1206
34. Nikawa, J. and Yamashita, S. (1992), *Mol. Microbiol*. 6, 1441-1446
35. Nikawa, J., Akiyoshi, M., Hirata, S. and Fukuda, T. (1996) *Nucleic Acids Res*. 2L4, 4222-4226
36. Nikawa, J., Murakami, A., Esumi, E and Hosaka, K. (1995) J. Biochem. 118, 39-45
37. Sriburi, R., Jackowski, S., Mori, K. and Brewer, J. W. (2005*) J. Cell Biol.* 167, 35-41
38. Bricker, J. H. and Walter, P. (2004) *PLoS Biol.* 2: e342
39. Wyles J. P. and Ridgeway, N. D. (2004) *Exp. Cell Res.* 297, 533-547
40. Lehto, M., Hynynen, R., Karjalainen, K., Kuismanen, E., Hyvarinen, K. and Olkkonen, V. M. (2005) *Exp. Cell Res*. 310, 445-462
41. Perry, R. J. and Ridgway, N. D. (2006) *Mol. Biol. Cell. in press.*
42. Beh, C. T., Cool, L., Phillips, J. and Rine, J. (2001) *Genetis.* 157, 1117-1140
43. Berg, S., Starbuck, J., Torrelles, J. B., Vissa, V. D., Crick, D. C., Chatterjee, D. and Brennan, P. J. (2005) *J. Biol. Chem,* 280, 5651-5663
44. Schofield, C. M., Trudell, J. R. and Harrison, N. L. (2004) *Biochemistry* 43, 10058-10063

ACKNOWLEDGEMENT

We are indebted for Dr. Yasuo Ikeda for essential help. We are especially grateful to Ms. Takako Hiraki for essential assistance throughout the study. We thank Drs. John T. Potts Jr., Etsuro Ogata and Mr. Yoshiomi & Mrs. Yumi Tamai for indispensable support; Ms. H. Yanagisawa, M. Kimura, M. Nakajima, M. Akiyama and Y. Nakano for indispensable assistance; Ms. Tomo Yoshida-Nishimoto for essential cooperation; Dr. Dovie Wylie for expert assistance; Carl Zeiss Inc. for technical advice; and all members of the Departments of Pharmacology and Anatomy for essential cooperation. We thank Dr. Masayuki Miura of Tokyo Univ. and Dr. Victor Yu of National Univ. of Singapore for expression plasmids, and Dr. Neil Cashman of Toronto Univ. for NSC34 cells. This work was supported by a grant from Japan Society for the Promotion of Science.

*1Abbreviations used in this paper: ALS, amyotrophic lateral sclerosis; SMA, spinal muscular atrophy; VAPB, vesicle-associated membrane protein-associated protein B; VAPA, vesicle-associated membrane protein-associated protein A; VAPC, vesicle-associated membrane protein-associated protein C; VAMP, vesicle-associated membrane protein; SOD1, Cu/Zn-superoxide dismutase; EGFP, enhanced green fluorescent protein; HA, hemagglutinin; XBP1, X-box binding protein 1; IRE-1, inositol requiring enzyme 1; UPR, unfolded protein response; TMD, transmembrane domain; GST, glutathione-S-transferase; OSBP, oxysterol binding protein; ORP, oxysterol binding protein related protein,

Figure legends

Figure 1 VAPB structure

A) VAPB contains three conserved domains: the N-terminal major sperm protein domain, the middle coiled-coil domain, and the C-terminal transmembrane domain.

B) Schematic illustrations of VAP expression vectors. VAP proteins localize in synaptic vesicle membranes, ER, and the Golgi apparatus, via their C-terminal transmembrane domains (TMD). MSP, major sperm protein domain; SV, synaptic vesicle.

Figure 2 P56S mutation enhances insolubility and polyubiquitination of VAPB.

A) The P56S mutation enhanced polyubiquitination of VAPB. NSC34 cells expressing His6-Xpress tagged wt-VAPB or P56S-VAPB in association with HA-ubiquitin (Ub) were lysed with the RIPA buffer and the total cell lysates were immunoprecipitated with anti-Xpress antibody.

Inputs and immunoprecipitates (IP) were then immunoblotted with anti-HA antibody or anti-HisG antibody.

B) The P56S mutation increased the Triton-X100 insoluble fraction of VAPB protein. NSC34 cells were transfected with the vector encoding His6-Xpress tagged wt-VAPB or P56S-VAPB. The Triton-X100 soluble (sol.) and insoluble (insol.) fractions were immunoblotted with anti-VAPB-P antibody. The black and white arrows indicate the exogenous (exo.) and endogenous (endo.) VAPB.

C) D) COS7 cells were transfected with the vectors encoding N-terminally-EGFP-fused wt-VAPB (wt-EGFP) (C) or N-terminally-EGFP-fused P56S-VAPB (P56S-VAPB) (D). At 48 hr after transfection, the cells were fixed and immunostained with anti-calreticulin (ER marker), followed by visualization with Texas-Red conjugated secondary antibody.

E) F) G) Untransfected NSC34 cells (E) or cells transfected with pEF4/His-wt-VAPB (F) or cells transfected with pEF4/His-P56S-VAPB (G), lysed in 1% Triton-X100-MBS, were subjected to sucrose density gradient centrifugation analysis. Each fraction (350 μl) was numbered in a top-to-bottom-of-tube order. Endogenous VAPB, His6-Xpress-VAPB, calnexin (ER membrane marker), or calreticulin (ER marker) were probed with anti-VAPB-P antibody, anti-HisG antibody, anti-calnexin antibody or anti-calreticulin antibody, respectively. Percentages indicate sucrose concentrations. short; short chemoimmunofluorescent exposure, long; long chemoimmunofluorescent exposure, P; pellet.

Figure 3. Messenger RNA of XBP1 is spliced by activated IRE1 in UPR.

Under normal condition, splicing of XBP1 mRNA by IRE1 does not occur and immature XBP1 protein is produced. Under ER stress condition, splicing by IRE1 occurs, followed by expression of fluorescent Venus protein-fused XBP1. The XBP1-ΔDBD, a deletion mutant of XBP1 lacking the DNA-binding domain, is also spliced by IRE1 in the same manner.

Figure 4 wt-VAPB, but not P56S-VAPB triggers UPR.

A), B) Overexpression of wt-VAPB triggers UPR. As a control, NSC34 cells were transfected with the vector encoding XBP1-ΔDBD-Venus (XBP1) and untreated (no) or treated with 1 μM of Thapsigargin for 24 hr. For investigation of VAPB effect on UPR, NSC34 cells were transfected with the vector encoding XBP1-ΔDBD-Venus (XBP1) in association with the backbone vector (vec), the vector encoding wt-VAPB, or the vector encoding P56S-VAPB. A) Triton X100-soluble and insoluble fractions of lysates were immunoblotted with anti-FLAG, anti-VAPB-P, and anti-tubulin antibodies. Immunoblot analysis of the insoluble fraction with anti-tubulin antibody was performed using the same membrane used for detection of VAPB with anti-VAPB-P antibody. B) XBP1-Venus fluorescence was detected with the fluorescent microscope.

C) D) Neither VAMP1 nor VAMP2 induces UPR. NSC34 cells were cotransfected with the vector encoding XBP1-ΔDBD-Venus (XBP1) in association with the pEF4/His vector (vec), pEF4/His-wt-VAPB, pEF4/His-P56S-VAPB, pEF4/His-VAMP1, or pEF4/His-VAMP2. Immunoblot analysis of Triton X100-soluble lysates was performed with anti-FLAG antibody

for XBP1, anti-HisG antibody for VAPB and VAMP, and anti-tubulin antibody for tubulin. D) XBP1-ΔDBD-Venus fluorescence was analyzed with the fluorescent microscope.
E) The proline residue at the 56th position of VAPB is essential for UPR induction. NSC34 cells were cotransfected with pCAX-F-XBP-1-Venus (XBP1) with the pEF1-vector (vec.), pEF1-wt-VAPB (wt), pEF1-P56X-VAPB (X; S, A, K, D), P56del-VAPB (proline at 56th was deleted), or K87D/M89D-VAPB. Cell lysates, divided into soluble (sol) or insoluble (insol) fractions, were immunoblotted with anti-VAPB-P antibody (VAPB proteins) and anti-FLAG antibody (XBP1).
F) P56A-VAPB and P56del-VAPB show non-ER localization similar to P56S-VAPB. COS cells were transfected with the vectors encoding N-terminally-EGFP-fused P56A-VAPB (P56A-VAPB) or N-terminally-EGFP-fused P56del-VAPB (P56del-VAPB). At 48 hr after transfection, the cells were fixed and immunostained with anti-calreticulin (ER marker), followed by visualization with Texas-Red conjugated secondary antibody.

Figure 5 Small interfering RNA for VAPB attenuates UPR.
A) B) C) Small interfering RNA for VAPB attenuates UPR induction by DTT or Thapsigargin. NSC34 cells, cotransfected with the vector encoding XBP1-ΔDBD-Venus (XBP1) and pRNA-U6.1/Shuttle-vector (si-vec) or pRNA-U6.1/Shuttle-siVAPB (si-VAPB), were treated with 1mM DTT or 100nM Thapsigargin for 6 hr. A) Spliced XBP1-ΔDBD-Venus (XBP1) was visualized by immunoblot analysis with anti-FLAG antibody. Endogenous VAPB and tubulin were detected by immunoblot analysis with anti-VAPB-P antibody and anti-tubulin antibody. B) The signal intensity was measured with a densitometric apparatus called "NIH Image". vec; vector, VB; siRNA for VAPB, DTT; dithiothreitol, Thapsi.; Thapsigargin. C) XBP1-ΔDBD-Venus fluorescence was detected with the fluorescent microscopy.

Figure 6 P56S-VAPB keeps its interaction with synaptic vesicular proteins.
NSC34 cells were harvested for pulldown analyses at 48 hr after transfection. All pulldown assays were performed with glutathione-sepharose beads. The precipitates were then immunoblotted with anti-HisG antibody (to detect His6-Xpress tagged proteins)(top panels) or anti-GST antibody (to detect GST-tagged protein)(bottom panels).
A) wt-VAPB or P56S-VAPB forms a homodimer. NSC34 cells were cotransfected with the GST-encoding backbone vector (vec), the vector encoding GST-wt-VAPB or GST-P56S-VAPB in association with the vector encoding His6-Xpress-wt-VAPB or His6-Xpress -P56S-VAPB.
B) wt-VAPB or P56S-VAPB forms a heterodimer with wt-VAPA. NSC34 cells were cotransfected with GST-vec or the vector encoding GST-wt-VAPB or GST-P56S-VAPB in association with the vector encoding His6-Xpress-wt-VAPA or His6-Xpress-P56S-VAPA.
C) wt-VAPB or P56S-VAPB forms a heterodimer with VAMP1 or VAMP2. NSC34 cells were cotransfected with the GST-vec or the vector encoding GST-VAMP1 or GST-VAMP2 in association with the vector encoding His6-Xpress-wt-VAPB or His6-Xpress-P56S-VAPB.

Figure 7 P56S-VAPB specifically enhances the insolubility of co-expressed wt-VAPB.

(A)(B)(C)(D) NSC34 cells were cotransfected with the vector encoding His6-Xpress tagged wt-VAPB (HX-VAPB) (A), His6-Xpress tagged wt-VAPA (HX-VAPA) (B), His6-Xpress tagged VAMP1 (HX-VAMP1) (C) or His6-Xpress tagged VAMP2 (HX-VAMP2) (D) in association with pEF1-vector (vec), pEF1-wt-VAPB (wt), or pEF1-P56S-VAPB (P56S). The soluble and insoluble fractions of the cell lysates were subjected to immunoblot analysis with indicated antibody. His6-Xpress-tagged proteins, non-tagged VAPB, and actin were visualized by immunoblot analysis with anti-HisG antibody (top panels), anti-VAPB antibody (middle panels), and anti-actin antibody (bottom panels), respectively. Anti-VAPB antibody can only visualize overexpressed VAPB proteins.

E) NSC34 cells were cotransfected with the vector encoding His6-Xpress tagged wt-VAPB in association with the pEF1 vector (vec), pEF1-wt-VAPB (wt), pEF1-P56X-VAPB (X; S, A, K, D), pEF1-P56del-VAPB (proline at the 56th position was deleted) or pEF1-K87D/M89D-VAPB. Cell lysates were fractionated into soluble or insoluble fractions. His6-Xpress-wt-VAPB (HX-wt) was probed with anti-HisG antibody while non-tagged VAPBs exogenously expressed by the pEF1 vectors and endogenous VAPB were probed with anti-VAPB-P antibody (bottom panel, non-tag/endo.).

F) G) NSC34 cells were cotransfected with the vector encoding His6-Xpress-tagged wt-VAPB (wt) in association with the pEF1 vector (vec) or pEF1-P56S-VAPB (P56S). The cell lysates in the Triton-X100-MBS buffer were subjected to sucrose density gradient centrifugation analysis. Each fraction was numbered in a top-to-bottom-of-tube order. Percentages indicate sucrose concentrations. Non-tagged P56S-VAPB exogenously expressed by the pEF1 vectors as well as endogenous VAPB (non-tag/endo), His6-Xpress-wt-VAPB (HX-wt), calnexin (ER membrane marker), and calreticulin (ER marker) were probed with anti-VAPB-P antibody, anti-HisG antibody, anti-calnexin antibody, and anti-calreticulin antibody, respectively. short expo.; short chemoimmunofluorescent exposure, long expo.; long chemoimmunofluorescent exposure, P; pellet.

H) COS7 cells were transfected with the vectors encoding N-terminally-EGFP-fused wt-VAPB (wt-EGFP) in association with the pEF1 vector (vec) or pEF1-P56S-VAPB. At 48 hr after transfection, the cells were fixed and immunostained with anti-calreticulin (ER marker), followed by visualization with Texas-Red conjugated secondary antibody.

Figure 8 P56S-VAPB affects UPR in a dominant-negative manner.

A) B) NSC34 cells were cotransfected with the vector encoding XBP1-ΔDBD-Venus (XBP1) (1.5 μg/dish) in association with 1.5 μg of pEF1-vector (vec) or pEF1-P56S-VAPB (P56S). Forty-eight hr after transfection, the cells were untreated (no) or treated with 200nM of Thapsigargin (TG) for 6hr. Spliced XBP1-ΔDBD-Venus (XBP1) was visualized by immunoblot analysis with anti-FLAG antibody (A) or detected with the fluorescent microscopy (B). VAPB and tubulin were visualized by immunoblot analysis with anti-VAPB-P antibody or anti-tubulin antibody, respectively.

Figure 9 The P56S mutation enhances homodimerization of VAPB.

A) B) C) Pulldown assays were performed, as shown in Experimental procedures. Bottom panels indicate immunoblot analysis of GST-tagged proteins pulled down with glutathione sepharose. Top panels indicate immunoblot analysis of co-precipitated VAPB proteins.
A) NSC34 cells were cotransfected with the vector encoding GST (vec), GST-wt-VAPB full length (FL), or GST-wt-VAPB-ΔTMD (ΔTMD) in association with His6-Xpress-tagged wt-VAPB. The deletion of C-terminal TMD drastically weakened the homodimerization of VAPB.
B) NSC34 cells were cotransfected with the vector encoding GST (vec), GST-wt-VAPB (wt), or GST-P56S-VAPB (P56S) in association with the vector encoding His6-Xpress-P56S-VAPB-ΔTMD. The P56S-mutation enhanced the dimerization between VAPB and VAPB-ΔTMD.
C) NSC34 cells were cotransfected with the vector encoding GST (vec), GST-VAMP1 (VAMP1), or GST-VAMP2 (VAMP2) in association with the vector encoding His6-Xpress-tagged P56S-VAPB-ΔTMD. P56S-VAPB-ΔTMD did not bind to VAMP1 or VAMP2.

Figure1

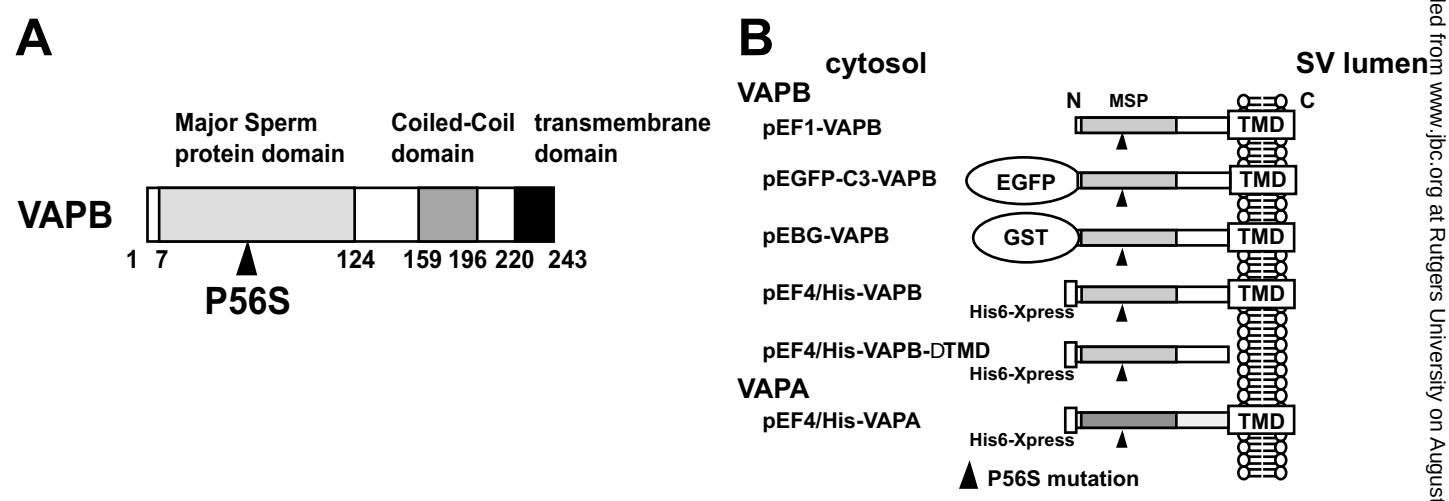

Figure2

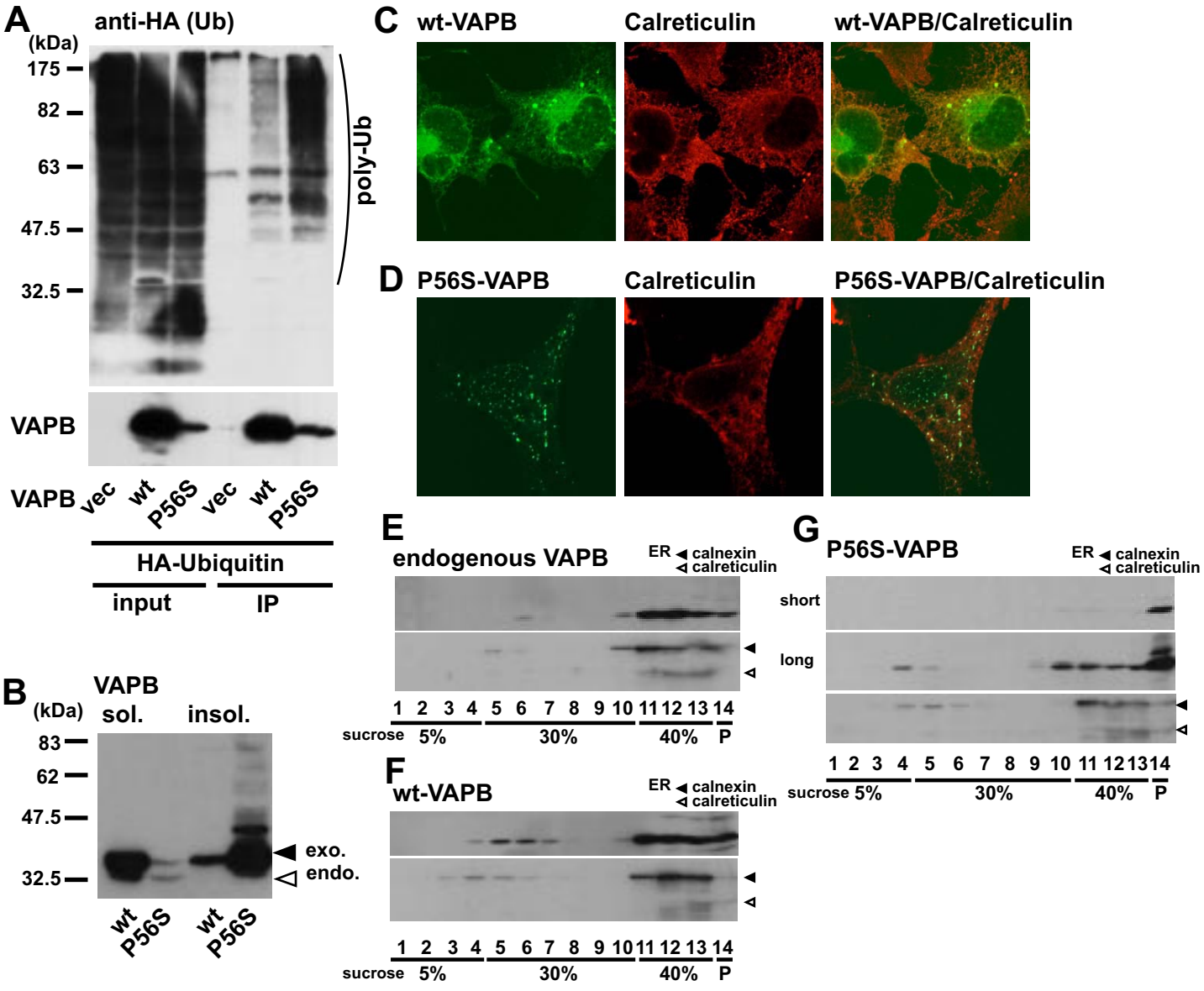

Figure 3

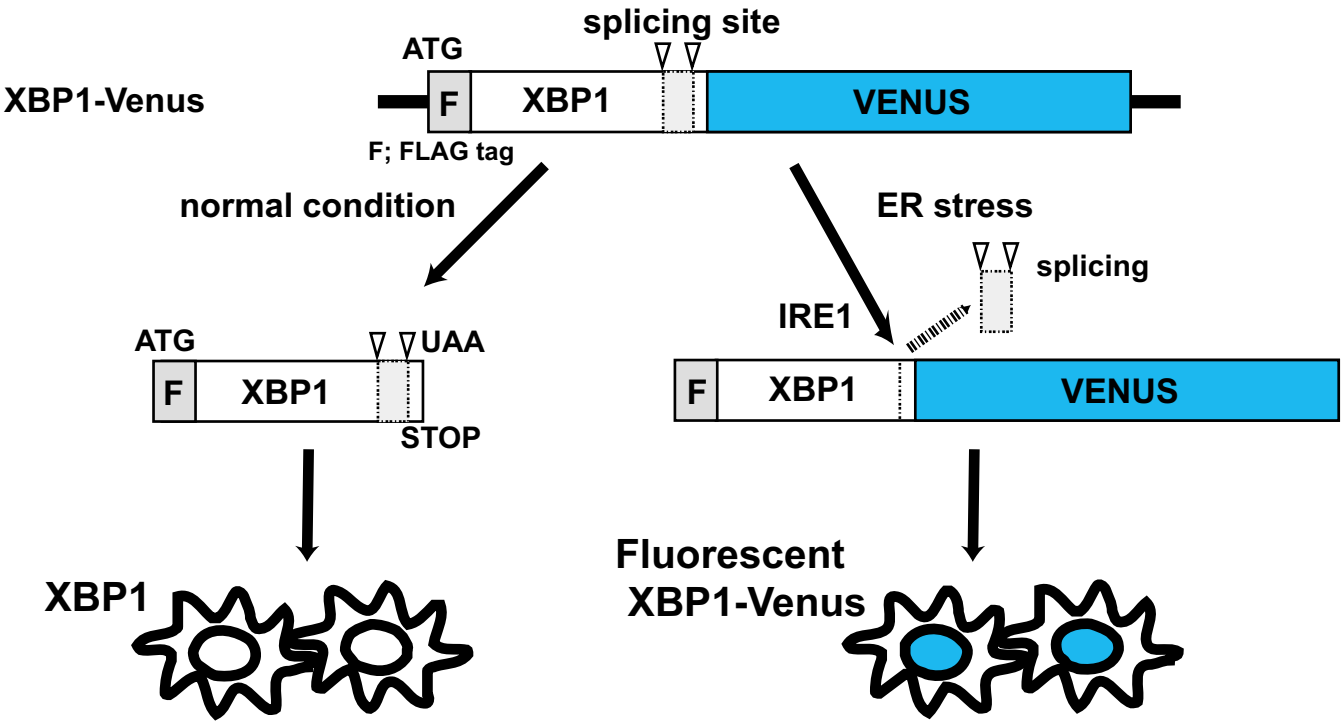

Figure 4

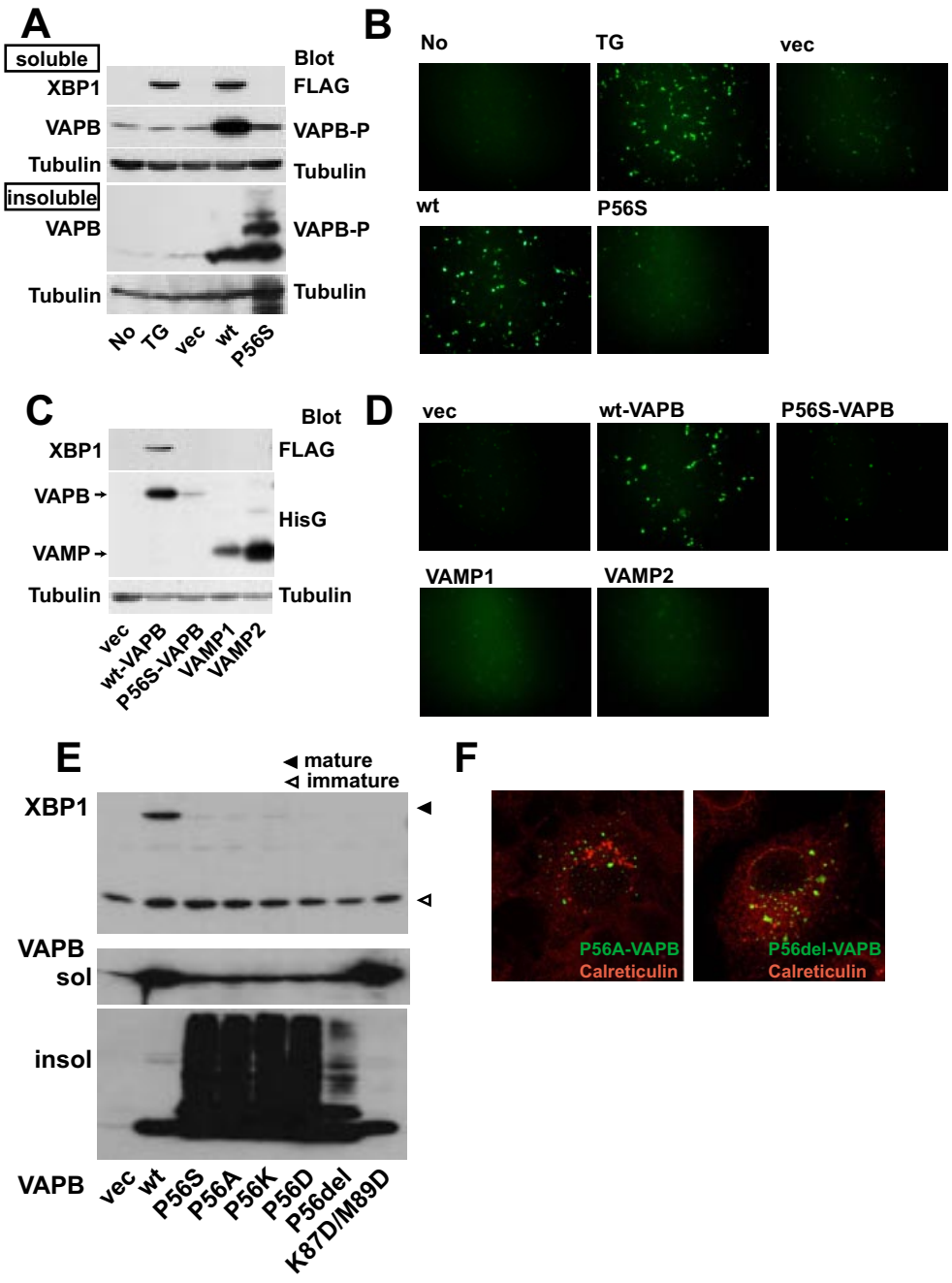

Figure 5

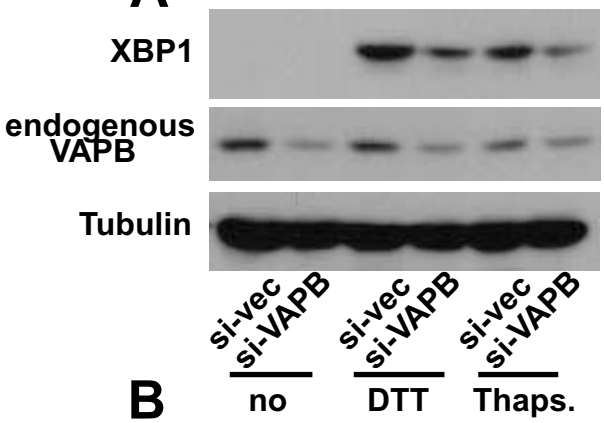

B

signal intensity

treat	NO		DTT		Thapsi.	
siRNA	vec	VB	vec	VB	vec	VB
XBP1	N.D.	N.D.	1.0	0.63	1.0	0.67
VAPB	1.0	0.51	1.0	0.56	1.0	0.86

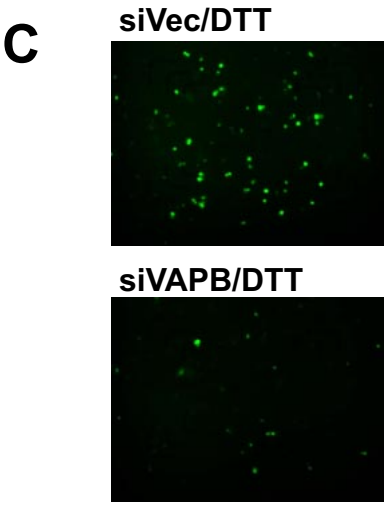

Figure 6

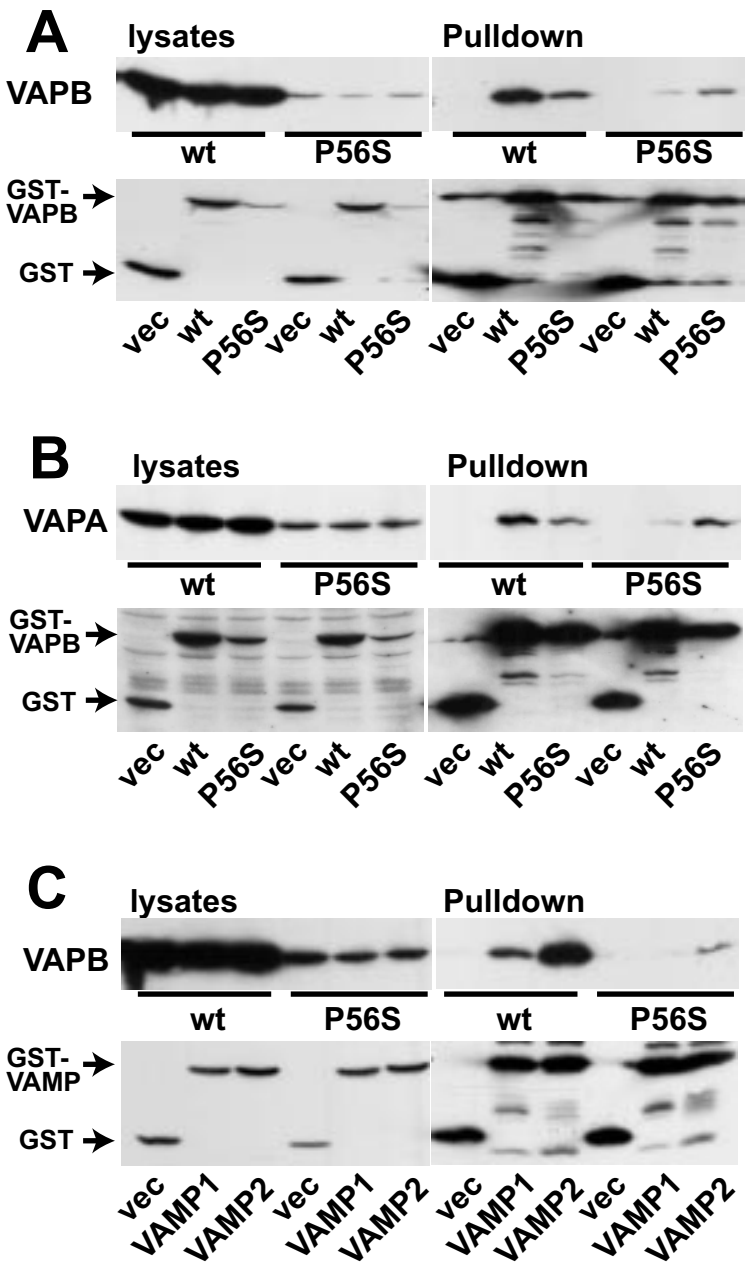

Figure 7

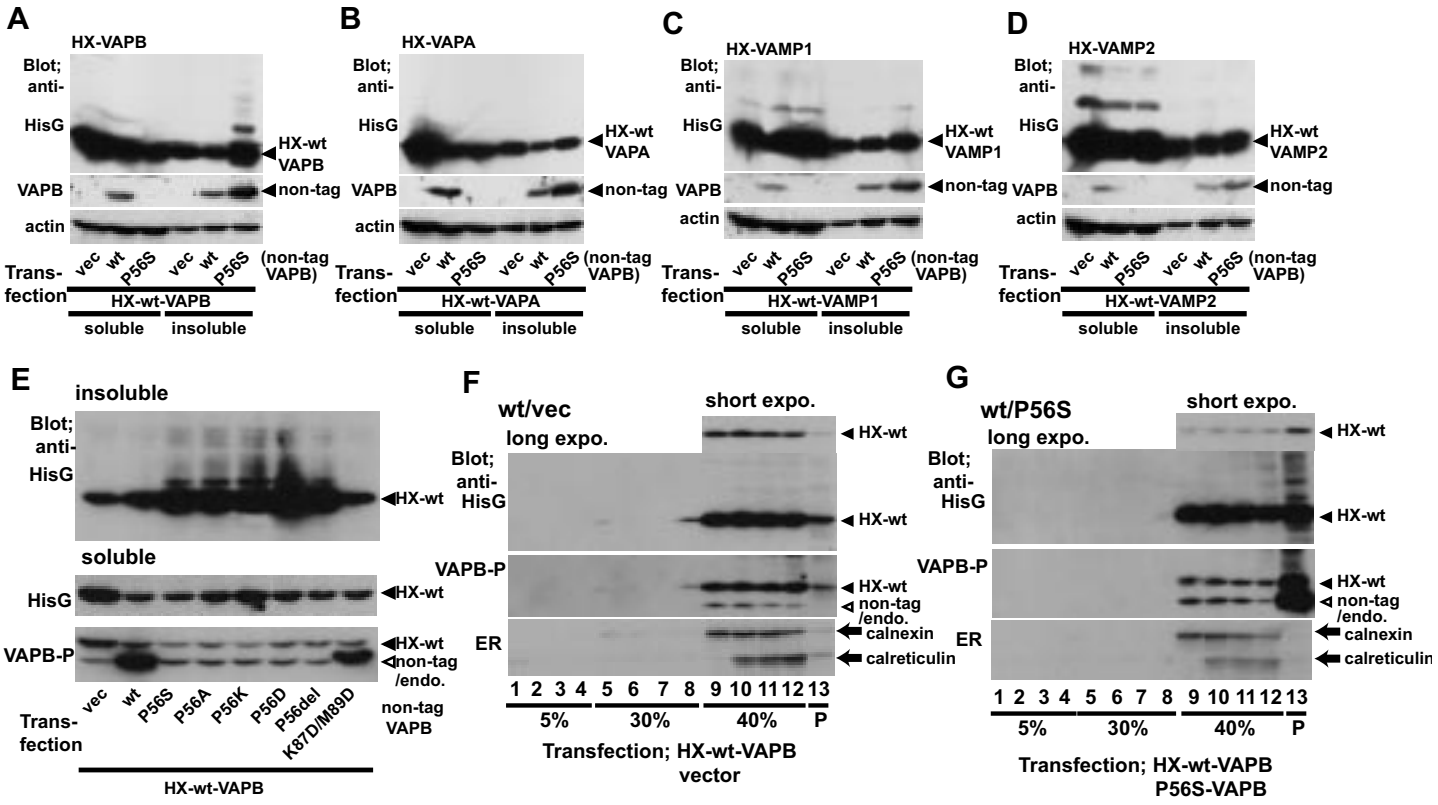

H

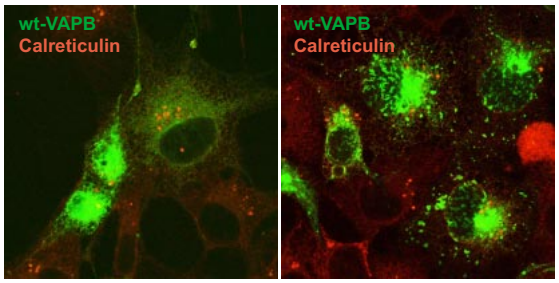

Figure 8

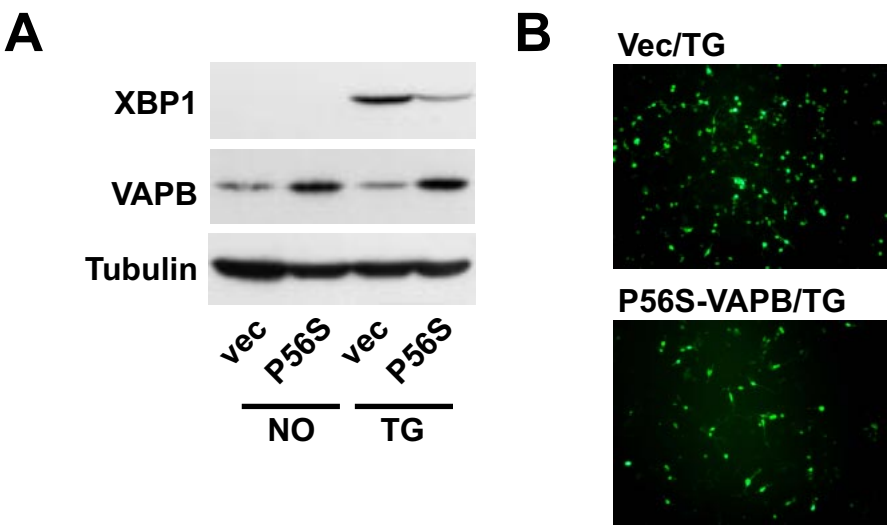

Figure 9